China Geology 6 (2023) 420−428

China Geology

Journal homepage: http://chinageology.cgs.cn
https://www.sciencedirect.com/journal/china-geology

$\delta^{13}C_{org}$ perturbations preserved by the interglacial Datangpo Formation in South China with implications for stratigraphic correlation and carbon cycle

Xian-yin An[a], Yu-jie Zhang[a,*], Li Tian[b], Shi-lei Liu[a], Qi-yu Wang[a], Yong Du[b], Hu-yue Song[b], Jun Hu[b]

[a] *Chengdu Center of China Geological Survey*, *Chengdu* 610081, *China*
[b] *State Key Laboratory of Biogeology and Environmental Geology*, *China University of Geosciences*, *Wuhan* 430074, *China*

ARTICLE INFO

Article history:
Received 30 May 2022
Received in revised form 17 November 2022
Accepted 15 December 2022
Available online 22 February 2023

Keywords:
Organic carbon isotope
Carbon cycle
Interglacial
Palaeoenvironmental reconstruction
Cryogenian Period
Snowball Earth
Neoproterozoic Era
Datangpo Formation
Geological survey engineering
South China Plate

ABSTRACT

Palaeoclimatic and palaeoenvironmental reconstructions of the Cryogenian Period have attracted attention in relation to the debated "Snowball Earth" hypothesis and the early evolution of metazoan life. The carbon cycle and redox conditions of the Sturtian-Marinoan non-glacial interval have been subjected to much controversy in the past decades because of the lack of a high-resolution stratigraphic correlation scheme. As one of the typical Sturtian-Marinoan interglacial deposits, the Datangpo Formation was widely distributed in South China with shales continuously deposited. The previous zircon dating data of the Datangpo Formation provide important ages for global constrain of the Sturtian-Marinoan non-glacial interval. Here we present a high-resolution straitigraphic study of the organic carbon isotopes of the Datangpo Formation from a drill core section in northern Guizhou Province. Based on measured episodic $\delta^{13}C_{org}$ perturbations, three positive shifts and three negative excursions are identified. A $\delta^{13}C_{org}$-based chemostratigraphic correlation scheme is proposed herein that works well for the Datangpo Formation regionally. Meanwhile, the $\delta^{13}C_{org}$ vertical gradients changed dynamically throughout the formation. This discovery implies that a significant ocean circulation overturn might have occurred in the upper Datangpo Formation, coinciding with the potential oxygenation.

1. Introduction

The occurrence of two global ice ages, the "Sturtian" and "Marinoan" glaciations, makes the Cryogenian Period (720 Ma to 635 Ma) one of the most climatically anomalous times in geological history (Macdonald FA et al., 2010). The "Snowball Earth" hypothesis proposed an extreme climatic condition with the Earth completely covered by ice (Hoffman PF et al., 1998), while the competing "Slushball Earth" hypothesis argues that there might have been some ice-free areas based on varied geochemical, sedimentological, and palaeontological evidence (Hyde WT et al., 2000; Allen PA and Etienne JL, 2008; Ye Q et al., 2015). In order to assess the spatial magnitude and temporal duration of these two glaciations and to understand their implications for biological events or the change of oceanic redox conditions, Sturtian-Marinoan interglacial successions have been intensively studied over the past decade (Corsetti FA et al., 2006; Hoffman PF et al., 2017).

Many authors have attempted to use carbonate carbon isotope-based chemostratigraphy on regional or/and global Cryogenian non-glacial strata correlations (Halverson GP et al., 2005; Macdonald FA et al., 2010; Swanson-Hysell NL et al., 2010; Johnston DT et al., 2012; Verdel C and Campbell M, 2017). However, only very limited $\delta^{13}C_{carb}$ and $\delta^{13}C_{org}$ measurements are available from the base of the shale-dominated Datangpo Formation of South China (Yu WC et al., 2017; Ai JY et al., 2021). Peng X et al. (2019) presented continuous high-resolution $\delta^{13}C_{org}$ profiles for the Datangpo/Xiangmeng Formation, showing significant $\delta^{13}C_{org}$ perturbations in shallow marine and deeper-water slope settings (Datangpo Formation), but a detailed correlation with global $\delta^{13}C$ profiles needs to be established. The most distinct $\delta^{13}C_{carb}$ excursion of the Cryogenian non-glacial successions, the "Trezona anomaly" (Halverson GP et al., 2005), hasn't been reported in South China yet. It is known that $\delta^{13}C_{carb}$ and

First author: *E-mail address*: axylw1988@163.com (Xian-yin An).

* Corresponding author: *E-mail address*: zhangyujie@mail.cgs.gov.cn (Yu-jie Zhang).

Literary editor: Xi-jie Chen
doi:10.31035/cg2022069
2096-5192/© 2023 China Geology Editorial Office.

$\delta^{13}C_{org}$ fluctuated throughout the Sturtian-Marinoan non-glacial interval, indicating significant palaeoclimatic and palaeoenvironmental changes such as warming/cooling, oceanic deoxygenation/oxygenation, and turnover of the carbon cycles. For decades, it has been argued whether temporal variation in $\delta^{13}C_{carb}$ and $\delta^{13}C_{org}$ of Cryogenian non-glacial intervals has been coupled or unpaired, but more comprehensive correlations are needed to fully understand this puzzling aspect of the carbon cycle (Swanson-Hysell NL et al., 2010; Johnston DT et al., 2012; Verdel C and Campbell M, 2017).

Here this paper presents a new high-resolution $\delta^{13}C_{org}$ profile throughout the Datangpo Formation to explore the significance of regional and global stratigraphic correlations and paleo-oceanic circulations.

2. Geological setting

Zircon dating analyses suggest that the ages and duration of the Sturtian and Marinoan glaciations might have been almost isochronous globally, with some differences between the duration of the glaciations in South China (Hoffman PF et al., 2017). With high-precision dating (zircon U-Pb CA-ID-TIMS), the duration of the Sturtian-Marinoan non-glacial interval has been established to span from 658.8 Ma to 654.5 Ma in South China (Zhang SH et al., 2008; Zhou CM et al., 2019), whilst the cyclostratigraphically constrained duration of the interglacial Datangpo Formation was about 9.8 Ma (Bao XJ et al., 2018).

The Neoproterozoic sedimentary basins in Hunan, Hubei, Chongqing and Guizhou are known as the Nanhua Basin, and the Yangtze-side of the Nanhua basin can be subdivided into the Hunan-Guangxi, the Jiangnan Ridge, and the northern Zhejiang sub-basins (Wang J and Li ZX, 2003). The Cryogenian successions of the Nanhua Basin in the Yangtze Block are generally quite varied, with three representative types (Zhou CM et al., 2016; Zhang YJ et al., 2020): (1) the mixtite-dominated Nantuo Formation is the only sedimentary representation of the Cryogenian in the western Hubei area; (2) the succession in the Hunan area consists of the Banxi Group (argillite), Gucheng (mixtite), Datangpo (shale), and Nantuo formations; (3) the sedimentary strata comprise Changan (mixtite), Fulu (siltstone), Tiesi'ao (mixtite), Datangpo, and Nantuo formations in the Guangxi area. Palaeogeographic analyses suggest that a bathyal sub-basin ran east-northward from Guangxi-Hunan to Zhejiang (Nanning-Changsha-Hangzhou, in the Fig. 1a), while the remaining parts of the Nanhua Basin represent basin shelf facies (Wang J and Li ZX, 2003).

Three lithological members in the shallow settings of the Datangpo Formation were recognized: Member I with massive carbonates, the shale-dominated Member II and siltstone-dominated Member III (in Yu WC et al., 2019). The thicknesses of these members vary significantly (Yu WC et al., 2016): (1) the basal carbonates are several meters thick (the known maximum is 15 m) at some localities whereas they are absent in other regions; (2) the total thickness of these members is about 50 m to hundreds of meters. In most local successions, there is no evidence for significant hiatuses of the Datangpo Formation, but the huge stratal thickness

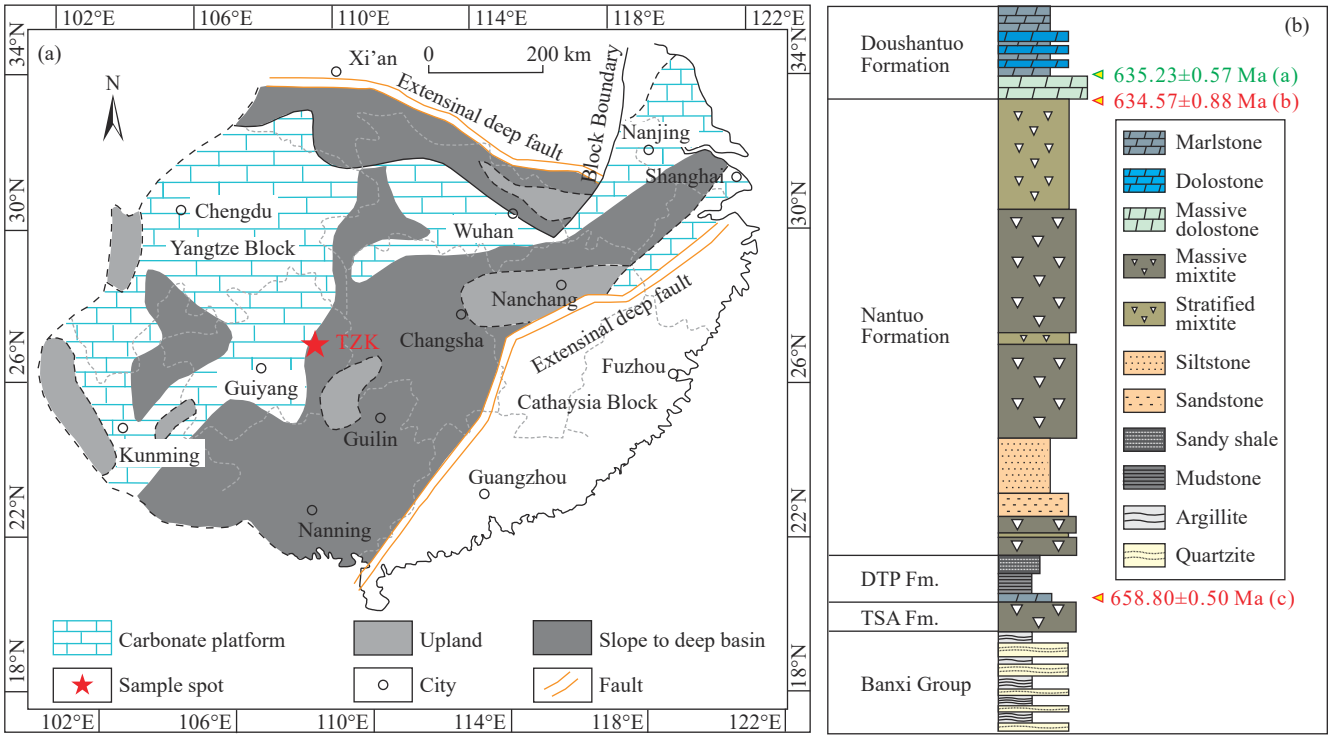

Fig. 1. Palaeogeographic location of the studied area and the regional Neoproterozoic lithological successions. (a) is modified from Ai JY (2021); (b) shows the general stratigraphic successions of the Hubei-Hunan-Chongqing-Guizhou area, modified from Hoffman PF and Li ZX (2009) while the dating data are from Condon D et al. (2005) and Zhou CM et al. (2019). DTP–Datangpo; TSA–Tiesi'ao; GC–Gucheng.

variations might be due to the palaeobathymetry of the Rift Basin (Yu WC et al., 2016).

The studied northwest-Guizhou and southeast Chongqing areas share the same succession with Hunan (Fig. 1b). Numerous cores have been drilled within this region during the past decades to detect manganese ore reserves. Many recent geochemical studies of the Datangpo Formation have been conducted with these drill core samples. The most famous of these is the Daotuo core, as it provides a series of data of Mo-U enrichment, magnetic susceptibility, and carbon isotopes (Ye YT et al., 2018; Bao XJ et al., 2018; Peng X et al., 2019). The drilled section of the TZK core in this study is located in Songtao County of the Guizhou Province (GPS: 28°13′06″ N, 109°04′10″ E), about 25 km southeast of the Daotuo section.

3. Methods

Lithostratigraphy was conducted in the field based on evident differences between underlying and overlying mixtites (Tiesi 'ao and Nantuo Formations) with their intervening shales. The carbonate beds are used as indicators for the basal Datangpo Formation, overlying the Tiesi 'ao Formation.

In total, 151 bulk samples were collected from the TZK drilled core (Fig. 2) throughout the Datangpo Formation for geochemical analyses. These samples were collected in varied sampling bins by lithological unit: (1) 0.5 m per sample of Member I: 15 samples; (2) 1 m per sample of Member II: 72 samples; (3) 10 m per sample of Member III: 64 samples. Veins were avoided to minimize possible hydrothermal effects and each sample was ground to powder by an automated mill equipped with a tungsten carbide chamber.

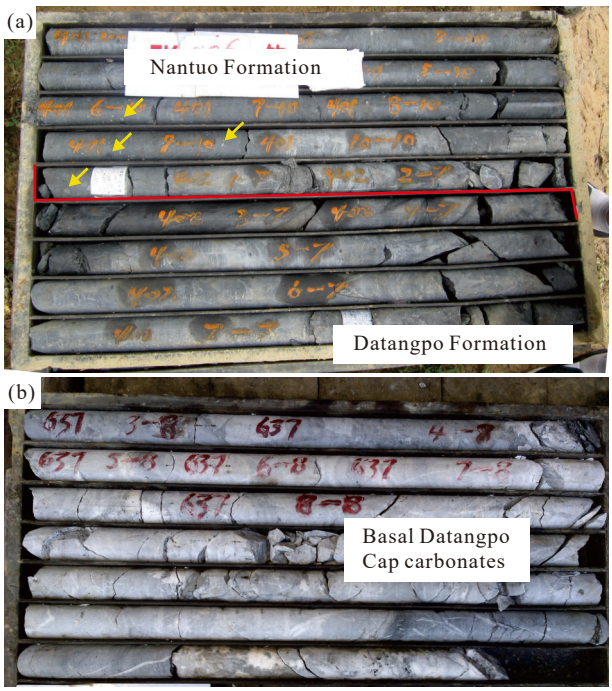

Fig. 2. Field photographs of the drilled core samples. a–uppermost Datangpo with the basal Nantuo Formations. The breccias of mixtite are shown with arrows. b–basal Datangpo cap carbonates, as the bottom of the drilled core section.

Carbon isotope measurements were conducted at the State Key Laboratory of Biogeology and Environmental Geology of the China University of Geosciences (Wuhan): (1) for the $\delta^{13}C_{carb}$ (and $\delta^{18}O_{carb}$) measurement of Member I, which is carbonate, about 1 g of powder from each sample was placed in a sealed Na-glass vial and reacted with pure phosphoric acid at 70°C after flushing with helium. The evolved CO_2 was analyzed using a Gasbench II coupled MAT 253 mass-spectrometer; (2) for the $\delta^{13}C_{org}$ measurements of all samples, 5 g of powder from each sample were dissolved in 3 N hydrochloric acid (at least 1 hour at 70°C) until carbonate minerals were completely removed. The remainder was rinsed at least three times with deionized water until it reached a neutral pH. about 40 mg of the dried remainder was analyzed using an EA-Delta V mass spectrometer. The presented $\delta^{13}C_{carb}$ and $\delta^{13}C_{org}$ values are standardized as δ values against the Vienna Pee Dee Belemnite standard (VPDB). Precision was better than 0.1‰ and 0.2‰ for $\delta^{13}C_{carb}$ and $\delta^{13}C_{org}$, respectively. In addition, the total organic carbon (TOC) contents of the bulk samples were analyzed by EA-IRMS along with $\delta^{13}C_{org}$ measurement, with analytical precision of approximately 0.05%.

4. Results

The $\delta^{13}C_{carb}$ values of Member I carbonates vary from −7.59‰ to −4.65‰ (mean: −5.71‰), whereas the $\delta^{13}C_{org}$ values are −33.95‰ to −30.87‰ (mean: −32.46‰). An evident $\delta^{13}C_{org}$ change occurred in the upper part of Member II at 65.75 m (cumulative thickness), recording a general increase from about −32‰ to −30‰ (Fig. 3; Table S1). It seems that the $\delta^{13}C_{org}$ values of Member III did not change as gradually as in the lower members, due to the 10–20 times lower sampling resolution. In order to establish an evenly sampled $\delta^{13}C_{org}$ profile, all raw data of members I and II are averaged in 10 m sampling bins (see discussion 5.2). The results show six distinctive excursions through the Datangpo Formation (marked as N1, N2 and N3 for the negative shifts, as well as P1, P2 and P3 for the positive shifts in Fig. 3).

TOC contents are significantly higher in the lowest 65.75 m of the Datangpo Formation, mostly varying from 1.4% to 3.0%, whilst overlying samples are much poorer in TOC, with values of <0.5%. The cross plot of TOC and $\delta^{13}C_{org}$ (Fig. 4) show a possible stabilizing $\delta^{13}C_{org}$ trend from high TOC (> 0.5%) to an extremely low $\delta^{13}C_{org}$ sample (TZK-41, −37.16‰; Fig. 3).

5. Discussion

5.1. Regional and global $\delta^{13}C_{org}$ stratigraphic correlations

High-resolution stratigraphic division and correlation schemes of the Datangpo Formation are to be established with more biostratigraphical and geochemostratigraphical proxies-. Recently, Peng X et al. (2019) reported continuous $\delta^{13}C_{org}$

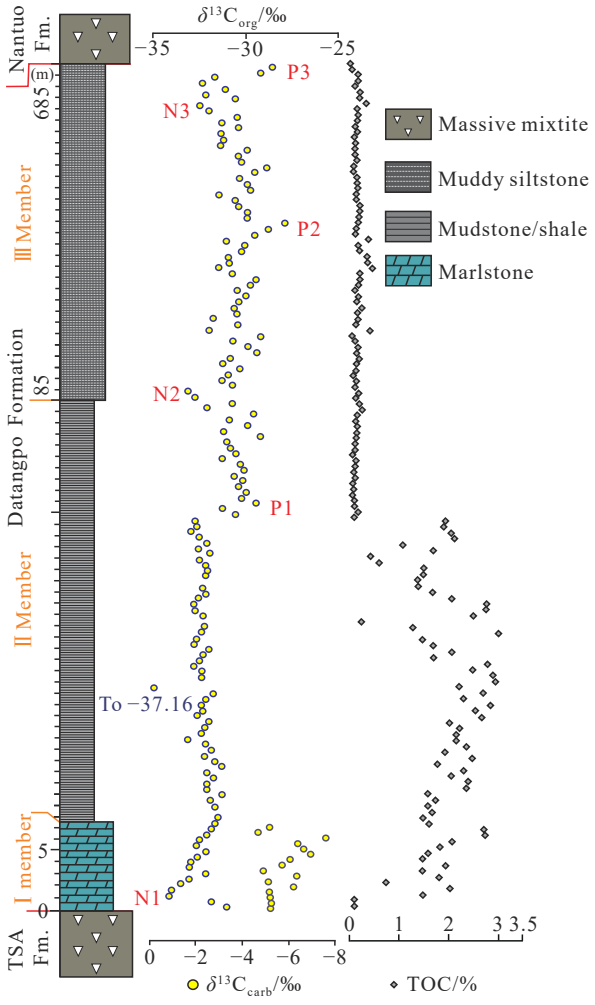

Fig. 3. Carbon isotopes and TOC contents profiles of the Datangpo Formation in the studied TZK section. Note: the thickness scales are varied in three members.

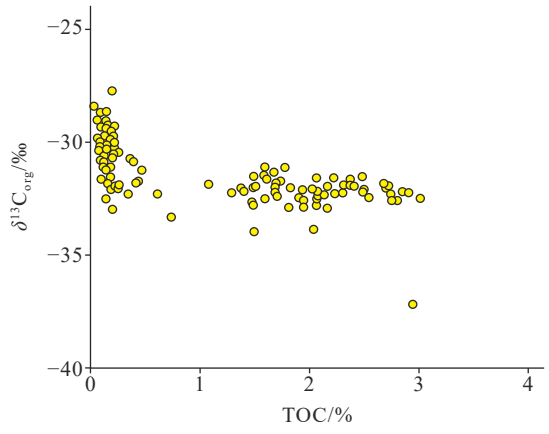

Fig. 4. Cross-plots of organic carbon isotopes and TOC contents of the studied Datangpo Formation in the TZK section.

data for three Sturtian-Marinoan sections in South China. The authors recognized evident negative $\delta^{13}C_{org}$ shifts in shallower settings (Datangpo Formation of the Daotuo and Minle sections) but failed to make detailed stratigraphic correlations in the absence of corresponding shifts in the deep setting (Xiangmeng Formation of the Xiangtan section). Compared to the identified $\delta^{13}C_{org}$ shifts in the TZK section, N1, P1, N2, P2, as well as N3, and P3 can all be identified in the Daotuo and Minle sections, but P3 is uncertain at Daotuo (Fig. 5).

Globally, higher resolution stratigraphic correlations of the Sturtian-Marinoan non-glacial interval were mainly based on $\delta^{13}C_{carb}$ of carbonate-dominated successions. Of the data collected in Scotland, South Australia, Namibia, Mongolia, and North America at least four distinctive $\delta^{13}C_{carb}$ excursions have been demonstrated to be potentially comparable (Fig. 6; Verdel C and Campbell M, 2017). Among these $\delta^{13}C_{carb}$ perturbations, an evident 10-20‰ negative shift occurred before the Marinoan Glaciation in Canada, Namibia, and Australia (Hoffman PF and Schrag DP, 2002). This negative shift was first termed the "Trezona anomaly" based on the large negative $\delta^{13}C_{carb}$ excursion in the Trezona Formation of South Australia (the N3 in the Fig. 6; McKirdy DM et al., 2001). The "Trezona anomaly" might have presented a global phenomenon, although it was not found in the Amadeus Basin (central Australia) and southwestern Mongolia (Verdel C and Campbell M, 2017). The absence of the "Trezona anomaly" in the Amadeus Basin might be due to the lack of continuous carbonate overlying the Limbla Formation, whereas the "Trezona anomaly" was discovered in the Trezona Formation of the nearby Adelaide Rift Complex (Swanson-Hysell NL et al., 2010) and the Flinders Ranges of South Australia (Klaebe R and Kennedy M, 2019). Although the $\delta^{13}C_{carb}$ and $\delta^{13}C_{org}$ values of the Trezona Formation in the Adelaide Rift Complex are decoupled, the $\delta^{13}C_{org}$ values of the "Trezona anomaly" are significantly lighter than in the underlying basal Etina Formation (Swanson-Hysell NL et al., 2010). Some researchers argued that the "Trezona anomaly", were possibly local event, invaliding $^{13}C_{carb.}$ of the "Trezona anomaly" as a global stratigraphic correlation indicator (Klaebe R and Kennedy M, 2019).

Here this study proposes that $\delta^{13}C_{org}$ can be used as a new chemostratigraphic correlation proxy in the Sturtian-Marinoan non-glacial interval, along with $\delta^{13}C_{carb}$. The $\delta^{13}C_{org}$-based stratigraphic correlation scheme we establish herein works well regionally for the Datangpo Formation of South China (Fig. 6) in deep settings (although the results were not convincing in the Xiangmeng Formation of the Xiangtan section because of the inter basin facies variances) and is likely to play a key role in future correlation as more continuous data from other basins become available. In contrast to $\delta^{13}C_{carb}$, which can only be employed in carbonate-dominated successions, $\delta^{13}C_{org}$ can be measured not only in carbonate strata, but also in clastic deposits (siltstone, mudstone, and shale), contributing to establishing a high-resolution and global-scale chemostratigraphic profile in varied sedimentary settings. Even in the carbonate continuous successions, $\delta^{13}C_{org}$-based stratigraphic division can be expected to shed some new light on global correlations. For example, in profiles of southwestern Mongolia no signs of N3, the "Trezona anomaly", were recognized based on $\delta^{13}C_{carb}$ data (Verdel C and Campbell M, 2017). However, a possible indication of N3 was shown by a distinct negative

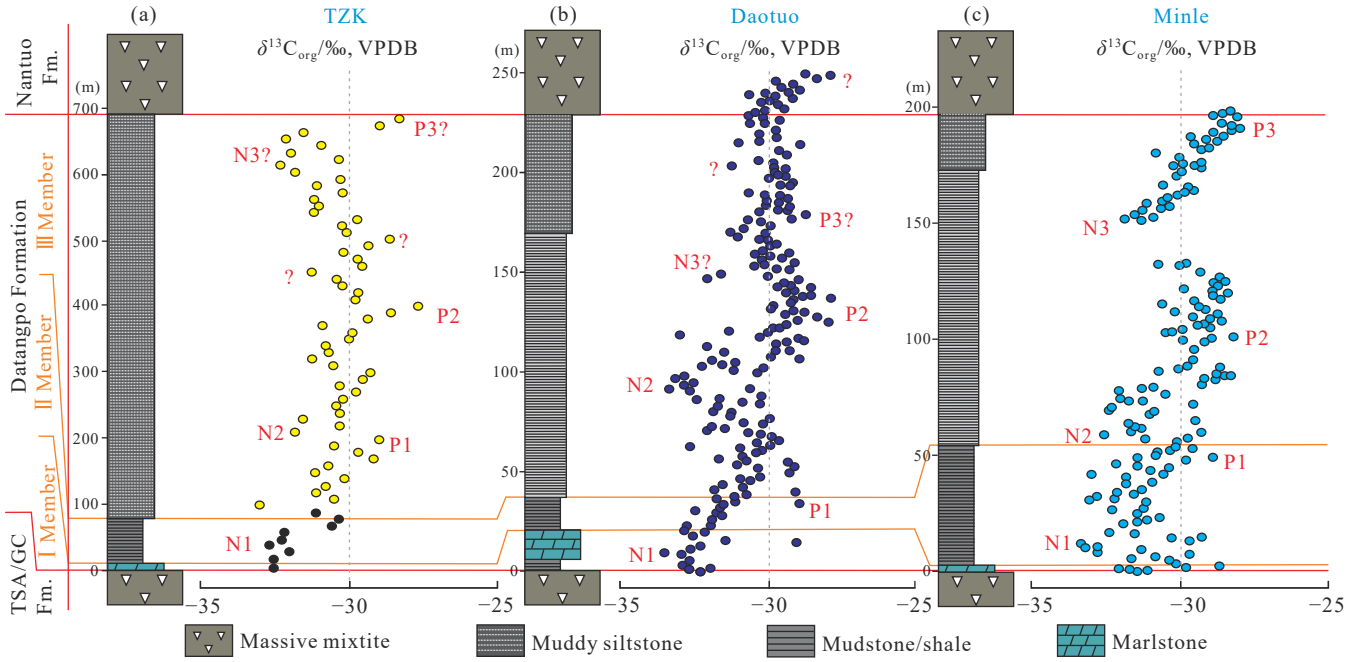

Fig. 5. Organic carbon isotope-based regional stratigraphic correlation of the Datangpo Formation. The raw data of TZK are from this study. Note that the open circles are averaged measurements with 10 m sampling bins. The original data of Daotuo and Minle are after Peng X et al. (2019).

shift of $\delta^{13}C_{org}$, although an additional $\delta^{13}C_{org}$ in the top of the Mongolian profile makes interpretation difficult (Fig. 6). It is worth to note that $\delta^{13}C_{carb}$ and $\delta^{13}C_{org}$ in the Cryogenian do not always covary (Swanson-Hysell NL et al., 2010). Kaufman AJ et al. (1997) reported coupled $\delta^{13}C_{carb}$ and $\delta^{13}C_{org}$ profiles from western Canada and Spitsbergen, although the profiles of the Rapitan-Ice Brook interval (Sturtian-Marinoan equivalent) are intermittent in terms of lithological variation (only N1, N2 and P2 were shown). Swanson-Hysell NL et al. (2010) demonstrated that the co-evolving $\delta^{13}C_{carb}$ and $\delta^{13}C_{org}$ were decoupled during the Sturtian-Marinoan non-glacial interval in Australia, most evidently in N3. However, this scenario was argued with different results from Mongolia and northwest Canada (Johnston DT et al., 2012). In Johnston's report, N1, P1, N2 and P2 were perfectly coupled in Mongolia (Fig. 6), whilst their presented data of $\delta^{13}C_{carb}$ and $\delta^{13}C_{org}$ from northwest Canada were too intermittent to make a full correlation. We cannot determine at present if this is also the case for $\delta^{13}C_{org}$. Future high-resolution $\delta^{13}C_{org}$ profiles from different Sturtian-Marinoan non-glacial successions are required to test this proposed correlation scheme at regional and global geographic scales.

5.2. Dynamic turnover of the carbon cycle

Controversies surrounding the nature of the carbon cycle of the Sturtian-Marinoan non-glacial interval have arisen because of these observed carbon isotopic inconsistencies. The decoupling of carbon isotopes was interpreted to have been caused by the growth of a large DOC pool at the onset of the Marinoan Glaciation (Swanson-Hysell NL et al., 2010), or riverine input of organic matter (Johnston DT et al., 2012). With the latest $\delta^{13}C_{org}$ profiles from the Datangpo Formation at hand, we support the deep marine DOC reservoir scenario because the $\delta^{13}C_{org}$ of the Datangpo Formation show correlative perturbations with the $\delta^{13}C_{carb}$ profiles of Africa, Australia and Scotland (Fig. 7), but realize that the carbon cycle was complicated by temporally varied oceanic conditions (e.g. redox, potential upwelling events; Peng X et al., 2019).

Along with the carbon isotopic profiles ($\delta^{13}C_{carb}$ or/and $\delta^{13}C_{org}$), $\Delta^{13}C$ gradients ($=\delta^{13}C^{shallow} - \delta^{13}C^{deep}$) play a key role in revealing the productivity and circulation of palaeo-oceans, and have already been successfully applied to Precambrian and Early Triassic deposits (Jiang GQ et al., 2007; Meyer KM et al., 2011; Song HY et al., 2013; Cheng M et al., 2021). Considering the huge sediment thickness and occurrence of the basal grainstone in TZK (section 4.1), the depositional environment should have been shallower than in the Minle and Daotuo areas. The organic carbon isotopic gradients are calculated with $\Delta N/P_n = \delta^{13}C\ (N/P_n^{TZK} - N/P_n^{Minle/Daotuo})$ with the method introduced by Luo GM et al. (2014). The results suggest that ΔN1, ΔN2 and ΔP2 are positive, whereas others are negative (ΔN3 and ΔP3) or absent (ΔP1) (Fig. 7a). The same result can also be observed in the Daotuo Section (Fig. 7b).

Reversed isotopic gradients (negative $\Delta^{13}C_{org}$ values) imply that the carbon fractionation mechanism may dynamically evolve. In the modern ocean, the isotopic gradient of organic carbon is very small or absent in well-oxygenated water masses and those with low terrigenous organic input (Benner R et al., 1997; Hernes PJ and Benner R, 2002). A positive $\Delta^{13}C_{org}$ excursion has been reported at the onset of the Permian-Triassic mass extinction, possibly

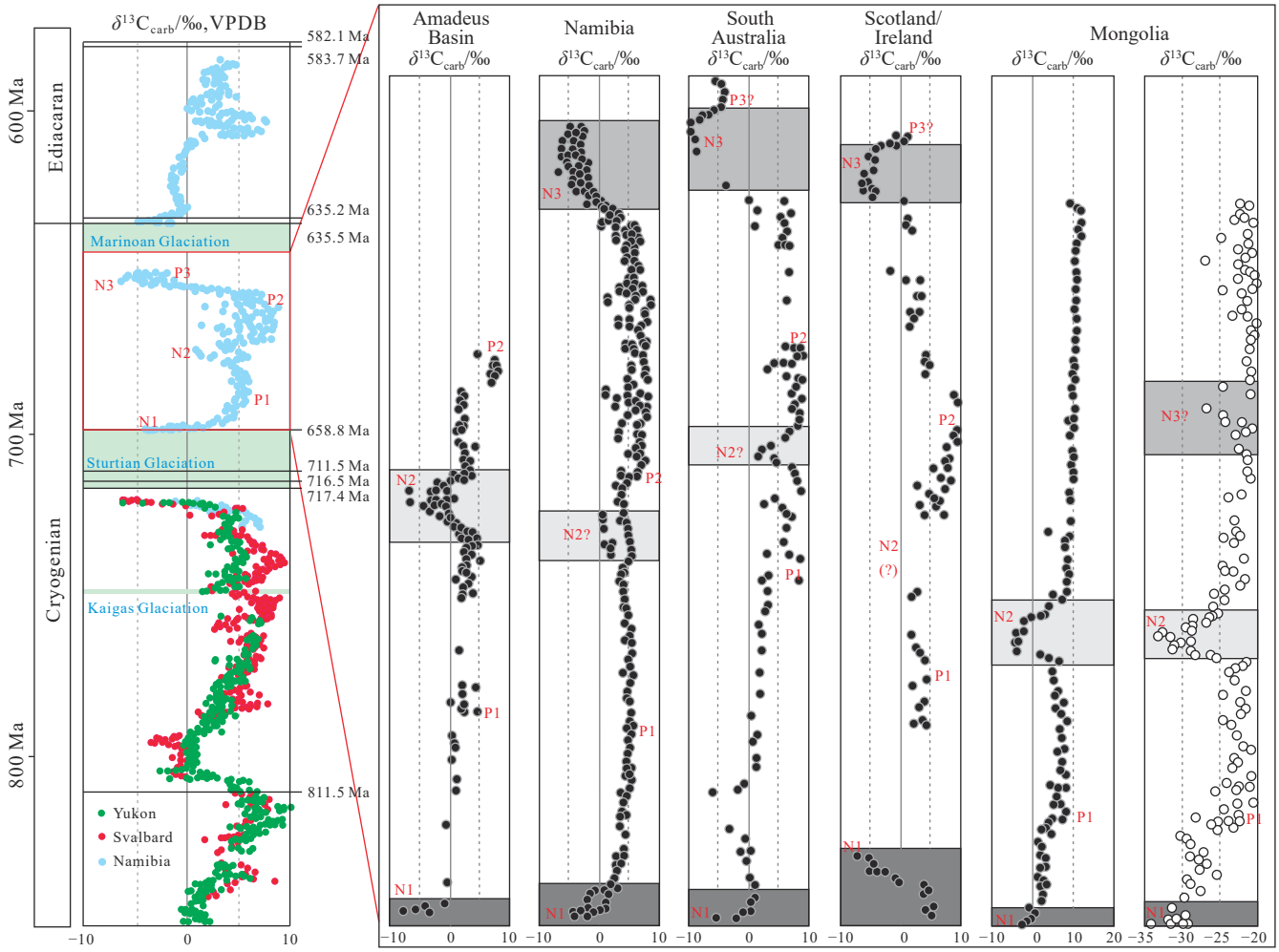

Fig. 6. Carbon isotope-based global stratigraphic correlations of the Sturtian-Marinoan interglacial interval. Following the correlation scheme proposed by Verdel C and Campbell M (2017), the three negative $\delta^{13}C_{carb}$ excursions are highlighted in gray: the N1 corresponds to the Rasthof excursion, N2 to the Taishir excursion and N3 to the Trezona excursion. The left composited Neoproterozoic $\delta^{13}C_{carb}$ curves are from Macdonald FA et al. (2010). The high precision dating data are from Macdonald FA et al. (2010) and Zhou CM et al. (2019). The right global correlations are simplified after Verdel C and Campbell M (2017) with additional data ($\delta^{13}C_{carb}$ and $\delta^{13}C_{org}$ of Mongolia) from Johnston DT et al. (2012).

caused by a bloom of microbes and dysoxia (Luo GM et al., 2014; Chen ZQ et al., 2022). Anoxia and a bloom of microbes in the basal Datangpo are supported by ample geochemical and sedimentary evidence (Feng LJ et al., 2010; Li C et al., 2012; Ye YT et al., 2018; Yu WC et al., 2019), and may be responsible for the ΔN1. The published geochemical data of the Minle section suggest that no significant redox change occurred during the N2 interval (Li C et al., 2012; Peng X et al., 2019), although Fe speciations show oxygenation in the N2 of the Daotuo section (Wei GY et al., 2020). Further investigations are required to decipher the potential redox related mechanism.

The Precambrian ocean is considered to have been comparative to oceans in the Permian-Triassic, whose redox conditions and carbon cycles have been intensively studied (Knoll AH et al., 1996). Negative $\Delta^{13}C_{org}$ were also observed in the immediate aftermath of the Permian-Triassic mass extinction in South China (Luo GM et al., 2014). The authors attempted to interpret the overturned $\Delta^{13}C_{org}$ of the Permian-Triassic transition as a consequence of planktonic community change (Luo GM et al., 2014). Many studies suggest that the immediate aftermath of the Permian-Triassic was associated with an oxygenation event rather than the expansion of anoxia (He L et al., 2013; Xiao YF et al., 2018). Peng X et al. (2019) interpreted the heavier $\delta^{13}C_{org}$ of the upper Datangpo in shallower settings as due to oxygenation of shallow water in a stratified ocean since the deeper Xiangtan section shows no significant isotopic variations. The geochemical evidence for redox reconstruction of the Yangjiaping, Minle and Daotuo sections also suggest an oxygenated environment in the upper Datangpo Formation (Li C et al., 2012; Wei GY et al., 2020).

6. Conclusion

A chemostratigraphic correlation scheme of the Datangpo Formations in South China is proposed based on episodic $\delta^{13}C_{org}$ excursions: three negative shifts (N1, N2, and N3) and three positive shifts (P1, P2 and, P3). The regional correlation works well in the Datangpo Formations with published data, but with imperfections in the indefinite P3 in the Datuo

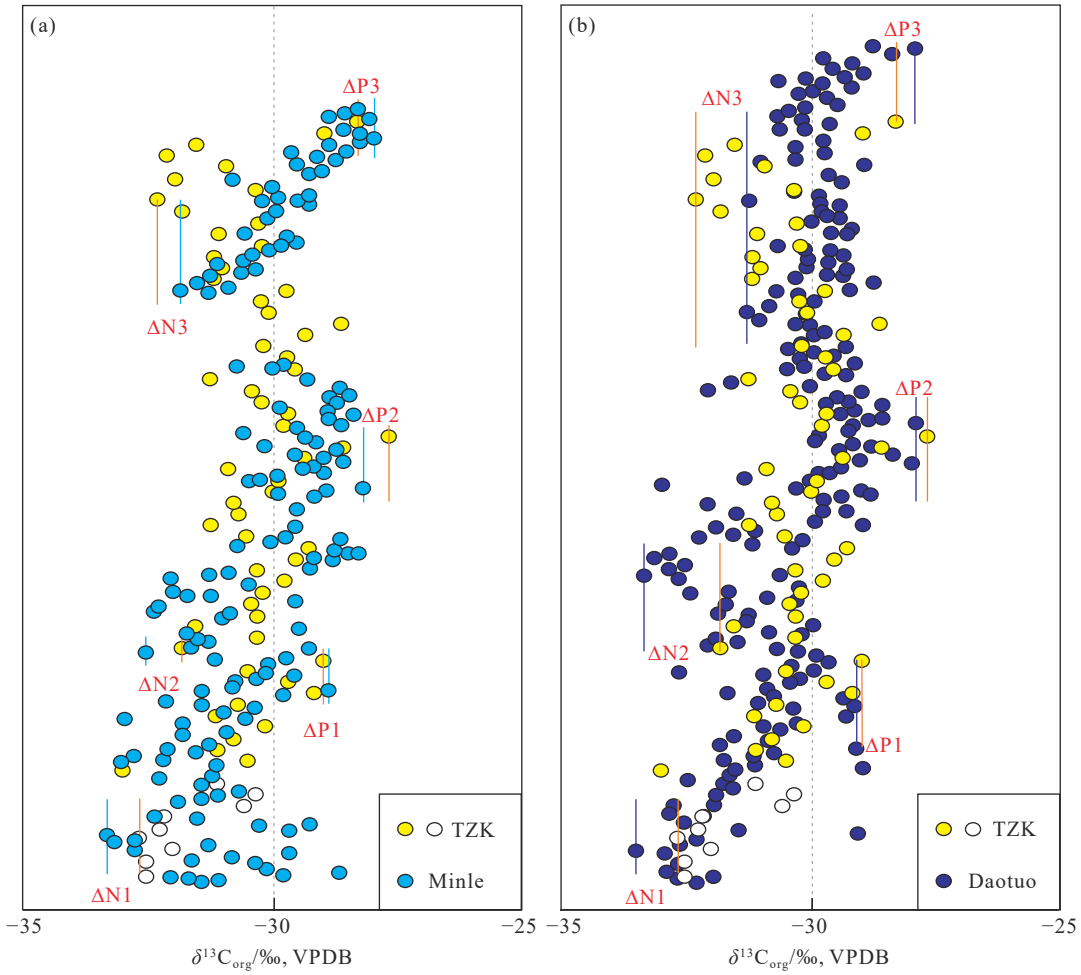

Fig. 7. Composited and correlated $\delta^{13}C_{org}$ of the Datangpo Formation from South China. ΔN/P = Max $\delta^{13}C_{org}$ − Min $\delta^{13}C_{org}$. The data sources and correlations are following Fig. 6.

section and invalidation in deeper settings (i.e. the Xiangmeng Formation). Additionally, the reversal of the $\delta^{13}C_{org}$ vertical gradients (ΔN3) discovered in the upper part of the Datangpo Formation suggests that a significant ocean circulation overturn might have occurred.

CRediT authorship contribution statement

Xian-yin An, Yu-jie Zhang and Li Tian conceived the presented idea. Xian-yin An and Li Tian prepared the manuscript. Yong Du, Hu-yue Song, and Jun Hu carried out the experiment. Shi-lei Liu and Qi-yu Wang contributed to sample preparation. All authors discussed the results and contributed to the final manuscript.

Declaration of competing interest

The authors declare no conflicts of interest.

Acknowledgments

Special thanks to Erik Tihelka for improving the English. This study was supported by the National Natural Science Foundation of China (41602126), the China Geological Survey (DD20160018, DD20221661), the Second Tibetan Plateau Scientific Expedition and Research Program (2019QZKK0706), and Liu Bao-jun Academician Research Funds subsidized by Chengdu Center of China Geological Survey.

Supplementary dataset

Supplementary data (Table S1) to this article can be found online at doi: 10.31035/cg2022069.

References

Ai JY, Zhong NN, Zhang TG, Zhang Y, Wang TG, George SC. 2021. Oceanic water chemistry evolution and its implications for post-glacial black shale formation: Insights from the Cryogenian Datangpo Formation, South China. Chemical Geology, 566, 120083. doi: 10.1016/j.chemgeo.2021.120083.

Allen PA, Etienne JL. 2008. Sedimentary challenge to Snowball Earth. Nature Geoscience, 1, 817–825. doi: 10.1038/ngeo355.

Bao XJ, Zhang SH, Jiang GQ, Wu HC, Li HY, Wang XQ, An ZZ, Yang TS. 2018. Cyclostratigraphic constraints on the duration of the Datangpo Formation and the onset age of the Nantuo (Marinoan) glaciation in South China. Earth and Planetary Science Letters, 483, 52–63. doi: 10.1016/j.epsl.2017.12.001.

Benner R, Biddanda B, Black B, McCarthy M. 1997. Abundance, size distribution, and stable carbon and nitrogen isotopic compositions of

marine organic matter isolated by tangential-flow ultrafiltration. Marine Chemistry, 57, 243–263. doi: 10.1016/S0304-4203(97)00013-3.

Chen ZQ, Fang YH, Wignall PB, Guo Z, Wu SQ, Liu ZL, Wang RQ, Huang YG, Feng XQ. 2022. Microbial blooms triggered pyrite framboid enrichment and oxygen depletion in carbonate platforms immediately after the latest Permian extinction. Geophysical Research Letters, doi: 10.1029/2021GL096998.

Cheng M, Zhang ZH, Algeo TJ, Liu SL, Liu XD, Wang HY, Chang B, Jin CS, Pan W, Cao MC, Li C. 2021. Hydroological controls on marine chemistry in the Cryogenian Nanhua Basin (South China). Earth-Science Reviews, 218, 103678. doi: 10.1016/j.earscirev.2021.103678.

Condon D, Zhu MY, Bowring S, Wang W, Yang AH, Jin YG. 2005. U-Pb ages from the Neoproterozic Doushantuo Formation, China. Science, 308, 95–98. doi: 10.1126/science.1107765.

Corsetti FA, Olcott AN, Bakermans C. 2006. The biotic response to Neoproterozoic snowball Earth. Palaeogeography, Palaeoclimatology, Palaeoecology, 232, 114–130. doi: 10.1016/j.Palaeo.2005.10.030.

Feng LJ, Chu XL, Huang J, Zhang QR, Chang HJ. 2010. Reconstruction of paleo-redox conditions and early sulfur cycling during deposition of the Cryogenian Datangpo Formation in South China. Gondwana Research, 18, 632–637. doi: 10.1016/j.gr.2010.02.011.

Halverson GP, Hoffman PF, Schrag DP, Maloof AC, Rice AH. 2005. Toward a Neoproterozoic composite carbon-isotope record. Geological Society of America Bulletin, 117, 1181–1207. doi: 10.1130/B25630.1.

He L, Wang YB, Woods A, Li GS, Yang H, Liao W. 2013. An oxygenation event occurred in deep shelf settings immediately after the end-Permian mass extinction in South China. Global and Planetary Change, 101, 72–81. doi: 10.1016/j.gloplacha.2012.12.008.

Hernes PJ, Benner R. 2002. Transport and diagenesis of dissolved and particulate terrigenous organic matter in the North Pacific Ocean. Deep Sea Research Part I:Oceanographic Research Papers, 49, 2119–2132. doi: 10.1016/S0967-0637(02)00128-0.

Hoffman PF, Kaufman AJ, Halverson GP, Schrag DP. 1998. A Neoproterozoic Snowball Earth. Science, 281, 1342–1346. doi: 10.1126/science.281.5381.1342.

Hoffman PF, Schrag DP. 2002. The snowball Earth hypothesis: Testing the limits of global change. Terra Nova, 14, 129–155. doi: 10.1046/j.1365-3121.2002.00408.x.

Hoffman PF, Li ZX. 2009. A palaeogeographic context for Neoproterozoic glaciation. Palaeogeography, Palaeoclimatology, Palaeoecology, 277 (2009), 158–172. doi: 10.1016/j.palaeo.2009.03.013.

Hoffman PF, Abbot DS, Ashkenazy Y, Benn DI, Brocks JJ, Cohen PA, Cox GM, Creveling JR, Donnadieu Y, Erwin DH, Fairchild IJ, Ferreira D, Goodman JC, Halverson GP, Jansen MF, Le Hir G, Love GD, Macdonald FA, Maloof AC, Partin CA, Ramstein G, Rose BEJ, Rose CV, Sadler PM, Tziperman E, Voigt A, Warrem SG. 2017. Snowball Earth Climate dynamics and Cryogenian geology-geobiology. Science Advances, 3, e1600983. doi: 10.1126/sciadv.1600983.

Hyde WT, Crowley TJ, Baum SK, Peltier WR. 2000. Neoproterozoic "snowball Earth " simulations with a coupled climate/ice-sheet model. Nature, 405, 425–429. doi: 10.1038/35013005.

Jiang GQ, Kaufman AJ, Christie-Blick N, Zhang SH, Wu HC. 2007. Carbon isotope variability across the Ediacaran Yangtze platform in South China: Implications for a large surface-to-deep ocean $\delta^{13}C$ gradient. Earth and Planetary Science Letters, 261, 303–320. doi: 10.1016/j.epsl.2007.07.009.

Johnston DT, Macdonald FA, Gill BC, Hoffman PF, Schrag DP. 2012. Uncovering the Neoprogerozoic carbon cycle. Nature, 483, 320–323. doi: 10.1038/nature10854.

Kaufman AJ, Knoll AH, Narbonne GM. 1997. Isotopes, ice ages, and terminal Proterozoic earth history. Proceeding of the National Academic of Sciences, 94, 6600–6605. doi: 10.1073/pnas.94.13.6600.

Klaebe R, Kennedy M. 2019. The palaeoenvironmental context of the Trezona anomaly in South Australia: do carbon isotope values record a global or regional signal? The depositional Record, 5, 131–146. doi:10.1002/dep2.60

Knoll AH, Bambach RK, Canfield DE, Grotzinger JP. 1996. Comparative Earth history and Late Permian mass extinction. Science, 273, 452–457. doi: 10.1126/science.273.5274.452.

Li C, Love GD, Lyons TW, Scott CT, Feng LJ, Huang J, Chang HJ, Zhang QR, Chu XL. 2012. Evidence for a redox stratified Cryogenian marine basin, Datangpo Formation, South China. Earth and Planetary Science Letter, 331/332, 246–256. doi: 10.1016/j.epsl.2012.03.018.

Luo GM, Algeo TJ, Huang JH, Zhou WF, Wang YB, Yang H, Richoz S, Xie SC. 2014. Vertical $\delta^{13}C_{org}$ gradients record changes in planktonic microbial community composition during the end-Permian mass extinction. Palaeogeography, Palaeoclimatology, Palaeoecology, 396, 119–131. doi: 10.1016/j.palaeo.2014.01.006.

Macdonald FA, Schmitz MD, Crowley JL, Roots CF, Jones DS, Maloof AC, Strauss JV, Cohen PA, Johnston DT, Schrag DP. 2010. Clibrating the Cryogenian. Science, 327, 1241–1243. doi: 10.1126/science.1183325.

McKirdy DM, Burgess JM, Lemon NM, Yu XK, Cooper AM, Gostin VA, Jenkins RJF, Both RA. 2001. A chemostratigraphic overview of the late Cryogenian interglacial sequence in the Adelaide Fold-Thrust Belt, South Australia. Precambrian Research, 106, 149–186. doi: 10.1016/S0301-9268(00)00130-3.

Meyer KM, Yu M, Jost AB, Kelley BM, Payne JL. 2011. $\delta^{13}C$ evidence that high primary productivity delayed recovery from end-Permian mass extinction. Earth and Planetary Science Letters, 302, 378–384. doi: 10.1016/j.epsl.2010.12.033.

Peng X, Zhu XK, Shi FQ, Yan B, Zhang FF, Zhao NN, Peng PA, Li J, Wang D, Shields GA. 2019. A deep marine organic carbon reservoir in the non-glacial Cryogenian ocean (Nanhua Basin, South China) revealed by organic carbon isotopes. Precambrian Research, 321, 212–220. doi: 10.1016/j.precamres.2018.12.013.

Song HY, Tong JN, Algeo TJ, Horacek M, Qiu HO, Song HJ, Tian L, Chen ZQ. 2013. Large vertical $\delta^{13}C_{DIC}$ gradients in Early Triassic seas of the South China craton: Implications for oceanographic changes related to Siberian Traps volcanism. Global and Planetary Change, 105, 7–20. doi: 10.1016/j.gloplacha.2012.10.023.

Swanson-Hysell NL, Rose CV, Calmet CC, Halverson GP, Hurtgen MT, Maloof AC. 2010. Cryogenian glaciation and the onset of carbon-isotope decoupling. Science, 328, 608–611. doi: 10.1126/science.1184508.

Verdel C, Campbell M. 2017. Neoproterozoic carbon isotope stratigraphy of the Amadeus Basin, central Australia. Geological Society of America Bulletin, 129, 1280–1299. doi: 10.1130/B31562.1.

Wang J, Li ZX. 2003. History of Neoproterozoic rift basins in South China: implications for Rodinian breakup. Precambrian Research, 122, 141–158. doi: 10.1016/S0301-9268(02)00209-7.

Wei GY, Wei W, Wang D, Li T, Yang XP, Shields GA, Zhang FF, Li GJ, Chen TY, Yang T, Ling HF. 2020. Enhanced chemical weathering triggered an expansion of euxinic seawater in the aftermath of the Sturtian glaciation. Earth and Planetary Science Letters, 539, 116244. doi: 10.1016/j.epsl.2020.116244.

Xiao YF, Wu K, Tian L, Benton MJ, Du Y, Yang H, Tong JN. 2018. Framboidal pyrite evidence for persistent low oxygen levels in shallow-marine facies of the Nanpangjiang Basin during the Permian-Triassic transition. Palaeogeography, Palaeoclimatology, Palaeoecology, 511, 243–255. doi: 10.1016/j.palaeo.2018.08.012.

Ye Q, Tong JN, Xiao SH, Zhu SX, An ZH, Tian L, Hu J. 2015. The survival of benthic macroscopic phototrophs on a Neoproterozoic snowball Earth. Geology, 43, 507–510. doi: 10.1130/G36640.1.

Ye YT, Wang HJ, Zhai LN, Wang XM, Wu CD, Zhang SC. 2018. Contrasting Mo-U enrichments of the basal Datangpo Formation in South China: implications for the Cryogenian interglacial ocean redox. Precambrian Research, 315, 66–74. doi: 10.1016/j.precamres.2018.07.013.

Yu WC, Algeo TJ, Du YS, Maynard B, Guo H, Zhou Q, Peng TP, Wang P, Yuan LJ. 2016. Genesis of Cryogenian Datangpo manganese deposit: Hydrothermal influence and episodic post-glacial ventilation of Nanhua Basin, South China. Palaeogeography, Palaeoclimatology, Palaeoecology, 459, 321–337. doi: 10.1016/j.palaeo.2016.05.023.

Yu WC, Algeo TJ, Du YS, Zhou Q, Wang P, Xu Y, Yuan LJ, Pan W. 2017. Newly discovered Sturtian cap carbonate in the Nanhua Basin, South China. Precambrian Research, 293, 112–130. doi: 10.1016/j.precamres.2017.03.011.

Yu WC, Polgári M, Gyollai I, Fintor K, Szabó M, Kovács I, Fekete J, Du YS, Zhou Q. 2019. Microbial metallogenesis of Cryogenian manganese ore deposits in South China. Precambrian Research, 322, 122–135. doi: 10.1016/j.precamres.2019.01.004.

Zhang SH, Jiang GQ, Han YG. 2008. The age of the Nantuo Formation and Nantuo glaciation in South China. Terra Nova, 20(4), 289–294. doi: 10.1111/j.1365-3121.2008.00819.x.

Zhang YJ, An XY, Liu SL, Gao YJ, Zheng J, Sang YH. 2020. The lithofaces, Mn- bearing sedimentary filling and palaeogeographic pattern of Early Datangpo Stage and implied for manganese in the northeastern Guizhou Province. Geology in China, 47(3), 607–626 (in Chinese with English abstract).

Zhou CM. 2016. Neoproterozoic lithostratigraphy and correlation across the Yangtze Block, South China. Journal of Stratigraphy, 40(2), 120–135 (in Chinese with English abstract).

Zhou CM, Huyskens MH, Lang XG, Xiao SH, Yin QZ. 2019. Calibrating the terminations of Cryogenian global glaciations. Geology, 47, 251–254. doi: 10.1130/G45719.1.